

## SUPPORTING INFORMATION

### Single-molecule magnet behavior in luminescent carbazoyl Dy(III) octahedral complexes with a quasi linear N<sup>-</sup>-Dy-N<sup>-</sup> angle.

Jérôme Long,<sup>\*a</sup> Alexander N. Selikhov,<sup>b, c</sup> Ekaterina Mamontova,<sup>a</sup> Konstantin A. Lyssenko,<sup>c, d</sup>  
Yannick Guari,<sup>a</sup> Joulia Larionova<sup>a</sup> and Alexander A. Trifonov<sup>\*b, c</sup>

<sup>a</sup> *Institut Charles Gerhardt, Equipe Ingénierie Moléculaire et Nano-Objets, Université de Montpellier, ENSCM, CNRS. Place Eugène Bataillon, 34095 Montpellier Cedex 5, France*

<sup>b</sup> *Institute of Organometallic Chemistry of Russian Academy of Sciences, 49 Tropinina str., GSP-445, 630950, Nizhny Novgorod, Russia. E-mail: trif@iomc.ras.ru*

<sup>c</sup> *Institute of Organoelement Compounds of Russian Academy of Sciences, 28 Vavilova str., 119334, Moscow, Russia.*

<sup>d</sup> *M.V. Lomonosov Moscow State University, Chemistry Department, Moscow, Russia 119991*

## TABLE OF CONTENTS

Experimental Section	3
General Procedure.	3
Synthesis of $[\text{DyR}_2(\text{py})_4][\text{B}(\text{C}_6\text{H}_5)_4] \cdot 2\text{py}$ (1).	3
Synthesis of $[\text{DyR}_2(\text{THF})_4][\text{B}(\text{C}_6\text{H}_5)_4](2)$ .	3
X-Ray crystallography.	3
Magnetic Measurements.	4
Photoluminescence measurements	4
Scheme S1: Synthesis of complexes 1 and 2. ....	5
Figure S1: Perspective view of the crystal packing for 1 and 2 along the <i>b</i> and <i>c</i> crystallographic axes, respectively. Hydrogen atoms have been omitted for clarity. ....	6
Figure S2: Temperature dependence of $\chi T$ under an applied magnetic field of 1000 Oe for 1 and 2. Inset: field dependence of the magnetization at 1.8 K for 1 and 2. ....	7
Figure S3: Hysteresis loops obtained at 1.8 K for 1 and 2 at an average sweep rate of 15 Oe.s <sup>-1</sup> . ....	7
Figure S4: Frequency dependence of $\chi'$ and $\chi''$ for 1 and 2 for different temperatures performed in zero magnetic static field. ....	8
Figure S5: Cole-Cole (Argand) plots obtained using the ac susceptibility data for 1 (right) and 2 (left) in zero magnetic field. The solid lines correspond to the best fit obtained with a generalized Debye model. ....	8
Figure S6: Temperature dependence of $\chi'$ and $\chi''$ for 1 for different frequencies performed in zero applied magnetic field. ....	9
Figure S7: Frequency dependence of $\chi'$ and $\chi''$ for 1 and 2 for various dc fields at 20 K. Right: Field dependence of the relaxation time for 1 at 6 K. The red solid line represents the fit with Eq. 2. ....	10
Figure S8: Field dependence of the relaxation time for 1 and 2 at 20 K. The red solid line represents the fit with Eq. 2. ....	10
Figure S9: Frequency dependence of $\chi'$ and $\chi''$ for 1 and 2 under a 1000 Oe dc field. ....	11
Figure S10: Cole-Cole (Argand) plot obtained using the ac susceptibility data for 1 (1000 Oe). The solid lines correspond to the best fit obtained with a generalized Debye model. ....	11
Figure S11: Orientation of the anisotropic axis (purple) in 1 and 2 obtained from the MAGELLAN software. ....	12
Figure S12: Room temperature emission spectrum for 1 (left) and 2 (right). ....	13
Figure S13: Excitation spectrum for 1 (left) and 2 (right). ....	13
Table S1: Crystal data, data collection and structure refinement details. ....	14
Table S2: SHAPE analysis for 1. ....	15
Table S3: Fitting of the Cole-Cole plots with a generalized Debye model for temperature ranging under a zero dc field for 1. ....	15
Table S4: Fitting of the Cole-Cole plots with a generalized Debye model for temperature ranging under a zero dc field for 2. ....	16
Table S5: Fit parameters of the field dependence of the relaxation time at 20 K for 1 and 2. ....	16
Table S6: Fitting of the Cole-Cole plots with a generalized Debye model under a 1000 Oe dc field for 1. ....	17
Table S7: Fitting of the Cole-Cole plots with a generalized Debye model under a 1000 Oe dc field for 2. ....	17
Table S8: Fit parameters of the temperature dependence of the relaxation time for 1 and 2. ....	18
Table S9: Fit parameters of the temperature dependence of the relaxation time for 1 and 2. ....	18

## EXPERIMENTAL SECTION

**General Procedure.** All operations were carried out under an atmosphere of argon using Schlenk techniques or in a nitrogen filled glovebox. After drying over KOH, THF was purified by distillation from sodium/benzophenone ketyl. Hexane and toluene were dried over Na/K alloy, transferred under vacuum, and stored in the glovebox. Pyridine was dried over CaH<sub>2</sub> and was degassed by freeze-pump-thaw methods, then condensed in a vacuum prior to use. Carbazole and [NHEt<sub>3</sub>][BPh<sub>4</sub>] were purchased from Aldrich and used without further purification. (o-Me<sub>2</sub>NC<sub>6</sub>H<sub>4</sub>CH<sub>2</sub>)<sub>3</sub>Dy was synthesized according to literature procedure.<sup>1</sup> Lanthanide metal analysis was carried out by complexometric titration.<sup>2</sup> IR spectra were recorded as Nujol mulls on a Bruker-Vertex 70 spectrophotometer. Elemental analysis was performed in the microanalytical laboratory of IOMC.

**Synthesis of [DyR<sub>2</sub>(py)<sub>4</sub>][B(C<sub>6</sub>H<sub>5</sub>)<sub>4</sub>]·2py (**1**).** [NHEt<sub>3</sub>][BPh<sub>4</sub>] (0.37 g, 0.88 mmol) was added to a yellow solution of (o-Me<sub>2</sub>NC<sub>6</sub>H<sub>4</sub>CH<sub>2</sub>)<sub>3</sub>Dy (0.50 g, 0.88 mmol) in toluene (10 mL) with vigorous stirring, after 10 minutes the solution turned orange and the borate dissolved. After 2 hours, carbazole (0.29 g, 1.76 mmol) was added to the solution and mixture was stirred for another 1 hour. Then all volatiles were removed in vacuum, and solid residue was dissolved in pyridine (3 mL). Large yellow crystals suitable for X-ray diffraction were obtained by slow diffusion of hexane into the py-solution of **1**. The yield of **1** is 0.94 g, 88%. Complex **1** crystallizes as a solvate with two molecules of pyridine. Elemental analysis calcd. (%) for C<sub>78</sub>H<sub>66</sub>BDyN<sub>8</sub> (1288.75 g/mol<sup>-1</sup>): C, 72.70; H, 5.16; N, 8.69; Dy, 12.61; found C, 72.45; H, 5.01; N, 8.36; Dy, 12.64. IR (Nujol, KBr) v/cm<sup>-1</sup>: 1638 (w), 1598 (s), 1579 (m), 1342 (w), 1327 (m), 1285 (w), 1241 (m), 1208 (s), 1151 (w), 1123 (w), 1062 (s), 1039 (m), 1003 (s), 919 (w), 895 (s), 844 (s), 700 (s), 628 (s), 609 (m).

**Synthesis of [DyR<sub>2</sub>(THF)<sub>4</sub>][B(C<sub>6</sub>H<sub>5</sub>)<sub>4</sub>](**2**).** The synthetic procedure is similar to that described for **1**. [NHEt<sub>3</sub>][BPh<sub>4</sub>] (0.37, 0.88 mmol), (o-Me<sub>2</sub>NC<sub>6</sub>H<sub>4</sub>CH<sub>2</sub>)<sub>3</sub>Dy (0.50 g, 0.88 mmol) and carbazole (0.29 g, 1.76 mmol). The solid residue was dissolved in THF (5 mL), colorless crystals of **2** were obtained by slowly cooling the solution from 65 to 20 °C. Yield of complex **2** is 0.82 g, 80%. Elemental analysis calcd. (%) for C<sub>64</sub>H<sub>68</sub>BDyN<sub>2</sub>O<sub>4</sub> (1102.57 g/mol<sup>-1</sup>): C, 69.72; H, 6.22; N, 2.54; Dy, 14.74; found C, 69.44; H, 6.04; N, 2.33; Dy, 14.64. IR (Nujol, KBr) v/cm<sup>-1</sup>: 1600 (s), 1327 (s), 1264 (w), 1238 (s), 1215 (w), 1161 (m), 1076 (m), 1034 (w), 1010 (w), 928 (m), 860 (w), 750 (s), 703 (s), 618 (m), 576 (m).

### X-Ray crystallography.

X-ray diffraction data for all studied complexes were collected on a SMART APEX II area-detector diffractometer (graphite monochromator,  $\omega$ -scan technique), using MoK $\alpha$ -radiation (0.71073 Å). The intensity data were integrated by the SAINT program<sup>1</sup> and were corrected for absorption and decay using SADABS<sup>3</sup> for the other complexes. All structures were solved by direct methods using SHELXS,<sup>4</sup> and were refined on F<sup>2</sup><sub>hkl</sub> using SHELXL-2014/2017.<sup>4-5</sup> All non-hydrogen atoms for the ordered part of the molecule were refined with anisotropic displacement parameters. All hydrogen atoms were placed in ideal calculated positions (C-H distance = 0.95 Å for aromatic hydrogen atoms) and refined as riding atoms with relative isotropic displacement parameters taken as Uiso(H)=1.2Ueq(C). The structures of **1** and **2** contained unresolved solvate molecules in the crystal

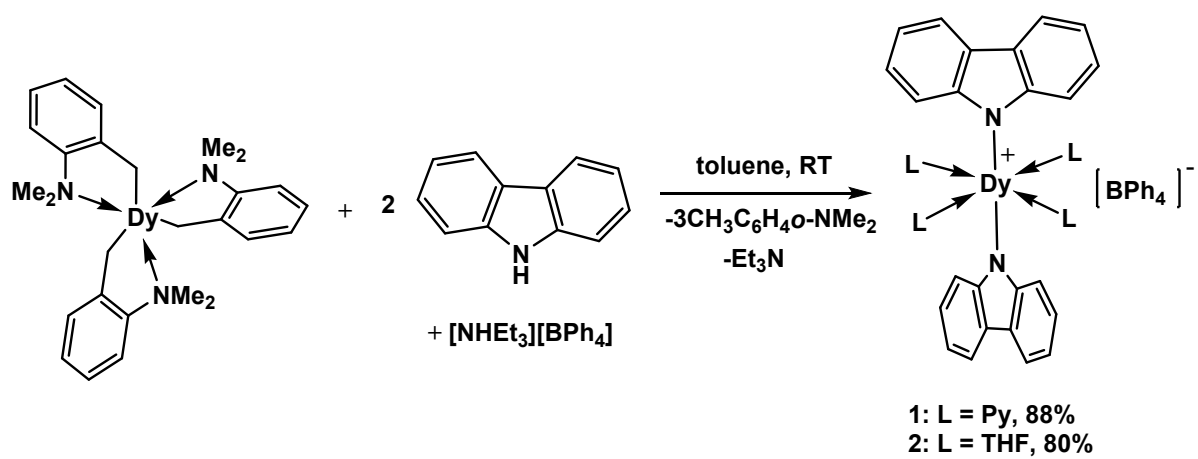
channels, which were removed by the SQUEEZE method<sup>6</sup> implemented in the PLATON program.<sup>7</sup> The SHELXTL program suite<sup>8</sup> was used for molecular graphics. Crystal data, data collection and structure refinement details are summarized in Table S1. CCDC 1972482-1972483 contain the supplementary crystallographic data for **1** and **2**. These data can be obtained free of charge via <http://www.ccdc.cam.ac.uk/conts/retrieving.html>, or from the Cambridge Crystallographic Data Centre, 12 Union Road, Cambridge CB2 1EZ, UK; fax: (+44) 1223-336-033; or e-mail: [deposit@ccdc.cam.ac.uk](mailto:deposit@ccdc.cam.ac.uk).

#### **Magnetic Measurements.**

Magnetic susceptibility data were collected with a Quantum Design MPMS-XL SQUID magnetometer working in the range 1.8 – 350 K with the magnetic field up to 7 Tesla. The sample were prepared in a glove box. The data were corrected for the sample holder and the diamagnetic contributions calculated from the Pascal's constants. The ac magnetic susceptibility measurements were carried out in the presence of a 3 Oe oscillating field in zero or applied external dc field.

#### **Photoluminescence measurements**

The solid sample was sealed in a quartz tube in an argon atmosphere (glove box). The emission and excitation spectra were recorded at 77 K and 295 K using a spectrofluorimeter Edinburgh FLS-920. The excitation source was a 450 W Xe arc lamp. The emission spectra were corrected for detection and optical spectral response of the spectrofluorimeter. Low temperature measurements (77 K) were performed using a liquid nitrogen dewar (quartz).



**Scheme S1:** Synthesis of complexes **1** and **2**.

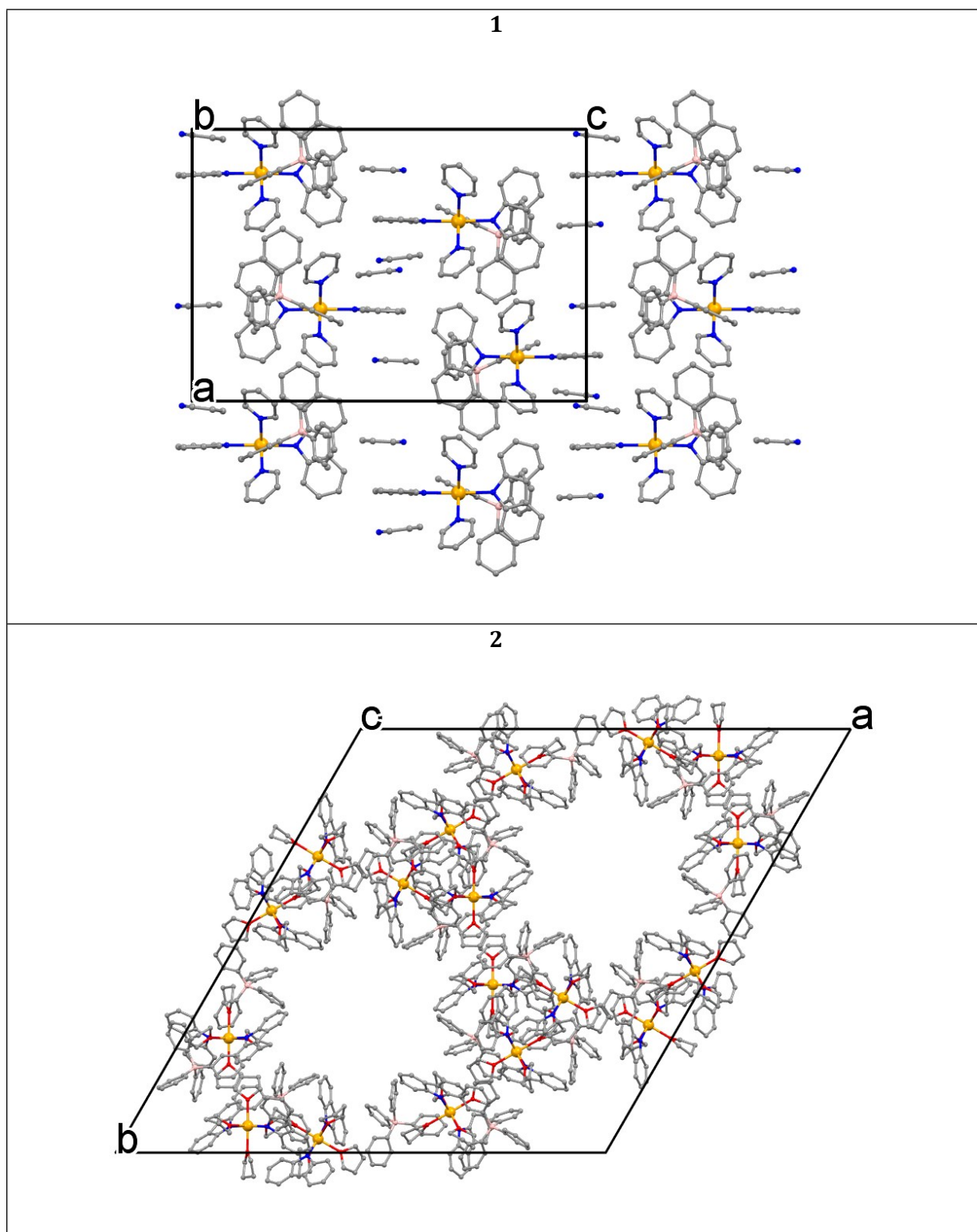


**Figure S1:** Perspective view of the crystal packing for **1** and **2** along the *b* and *c* crystallographic axes, respectively. Hydrogen atoms have been omitted for clarity.

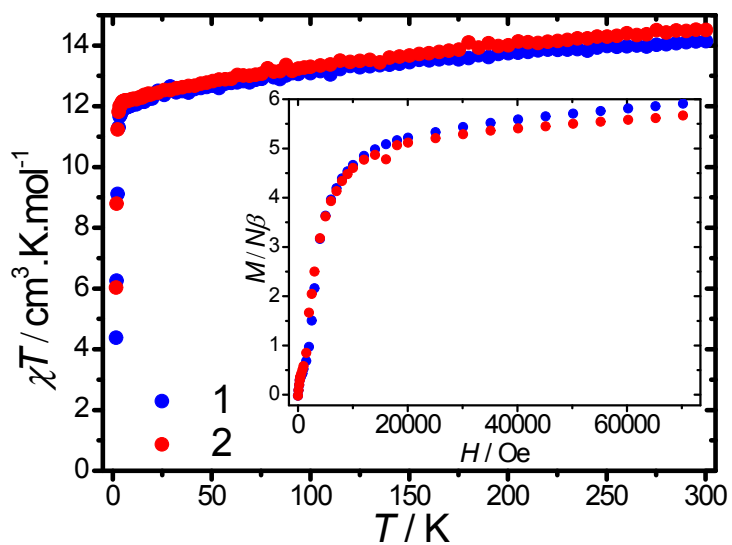


**Figure S2:** Temperature dependence of  $\chi T$  under an applied magnetic field of 1000 Oe for **1** and **2**.

Inset: field dependence of the magnetization at 1.8 K for **1** and **2**.

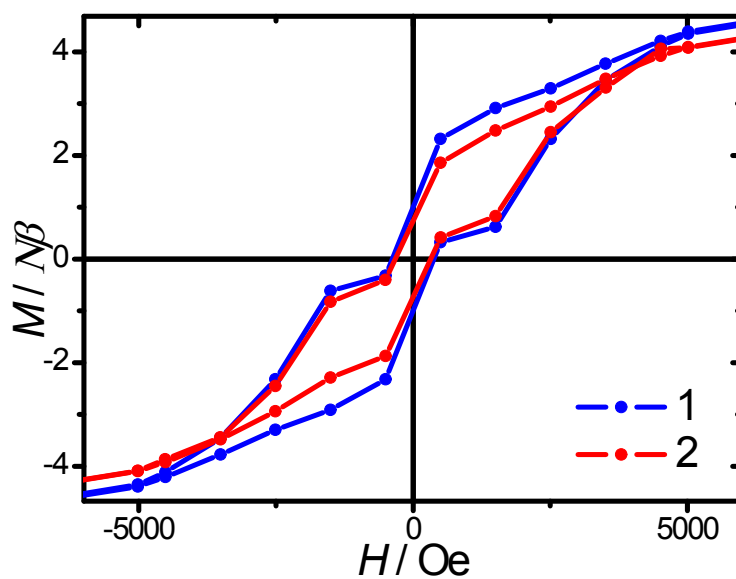


**Figure S3:** Hysteresis loops obtained at 1.8 K for **1** and **2** at an average sweep rate of  $15 \text{ Oe} \cdot \text{s}^{-1}$ .

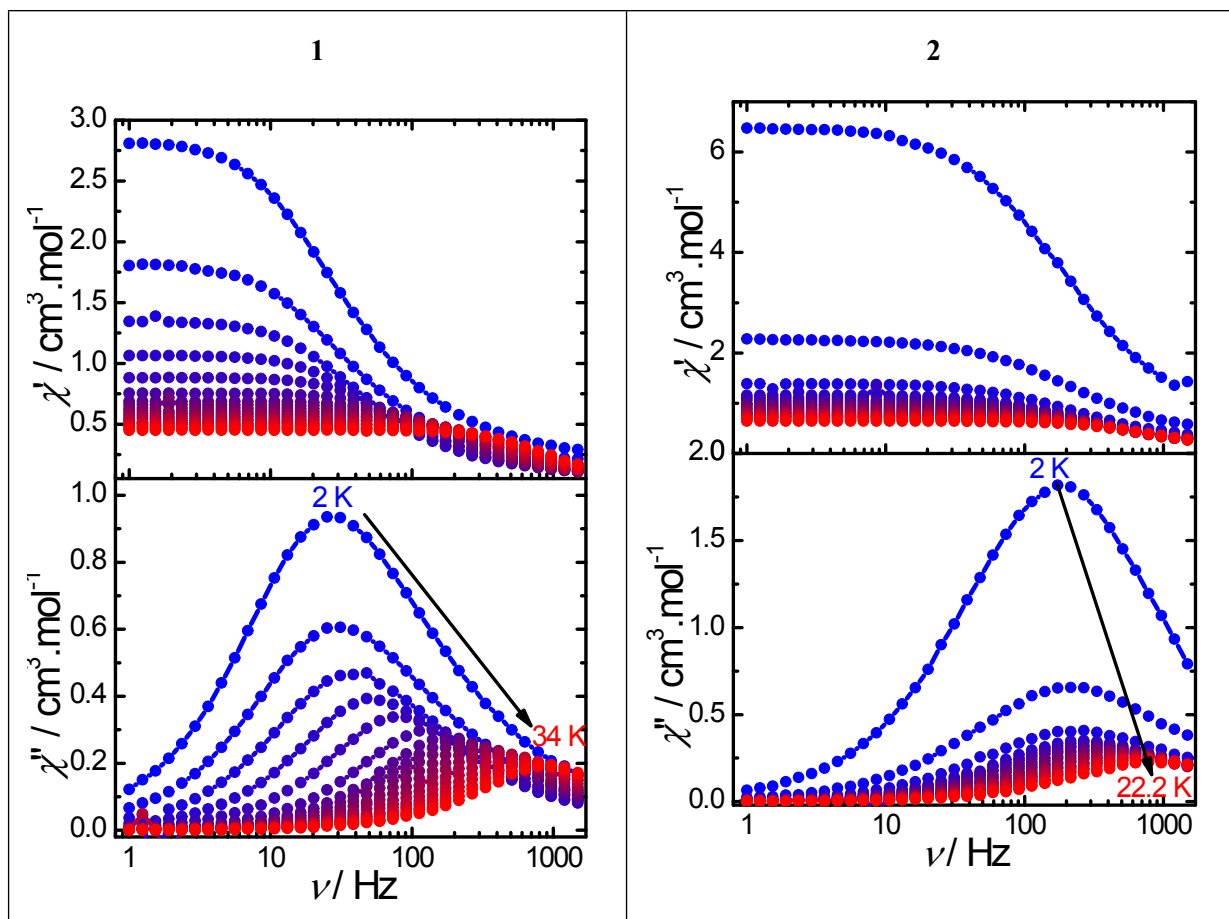


**Figure S4:** Frequency dependence of  $\chi'$  and  $\chi''$  for **1** and **2** for different temperatures performed in zero magnetic static field.

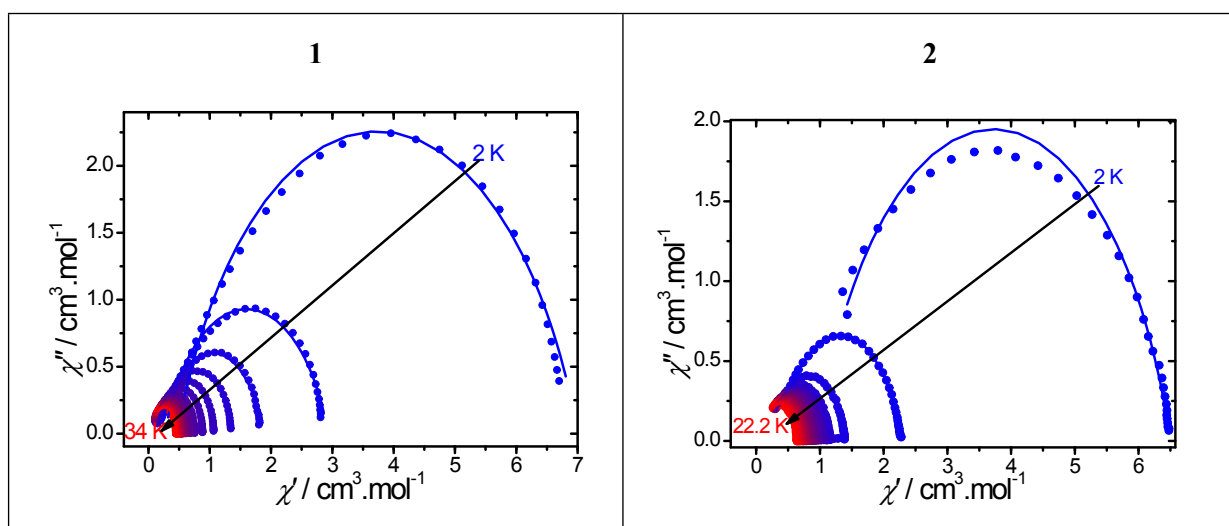


**Figure S5:** Cole-Cole (Argand) plots obtained using the ac susceptibility data for **1** (right) and **2** (left) in zero magnetic field. The solid lines correspond to the best fit obtained with a generalized Debye model.



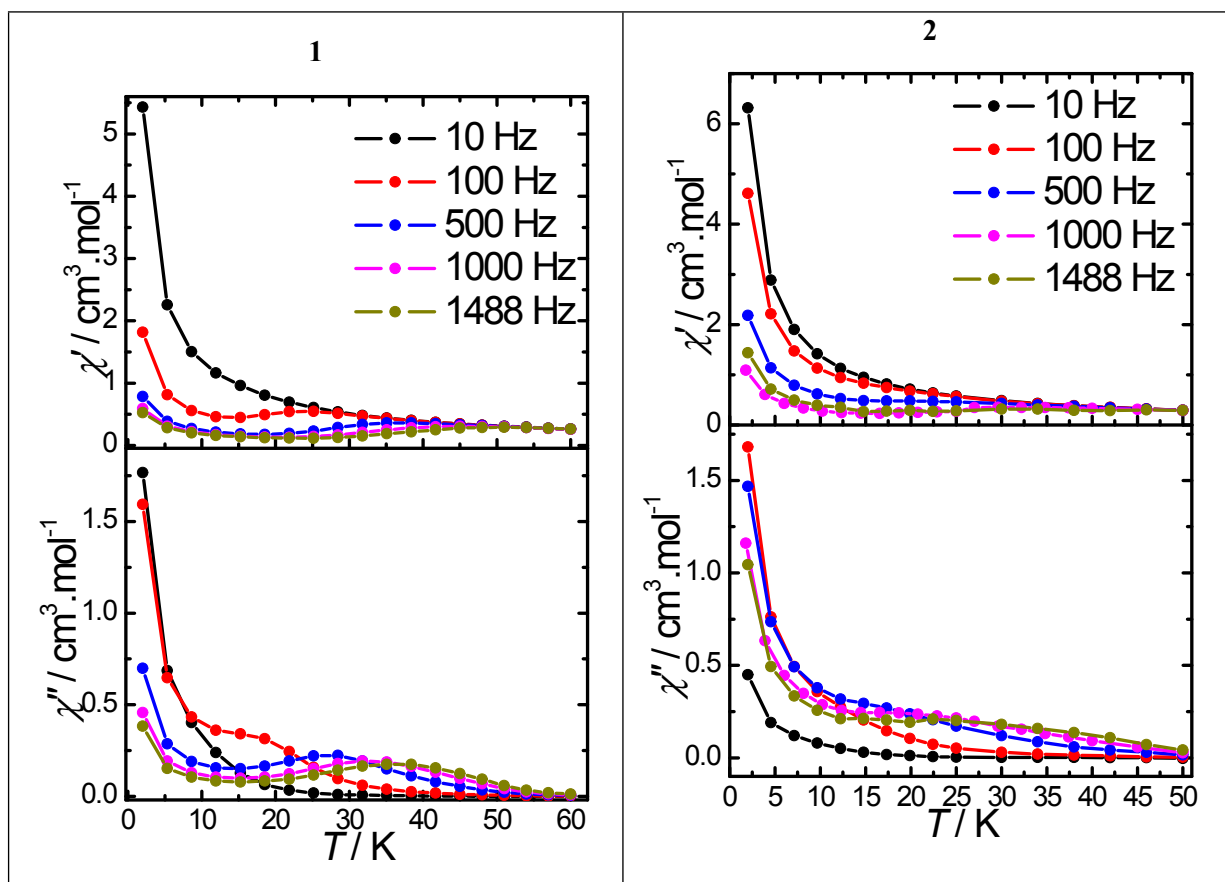


**Figure S6:** Temperature dependence of  $\chi'$  and  $\chi''$  for **1** for different frequencies performed in zero applied magnetic field.

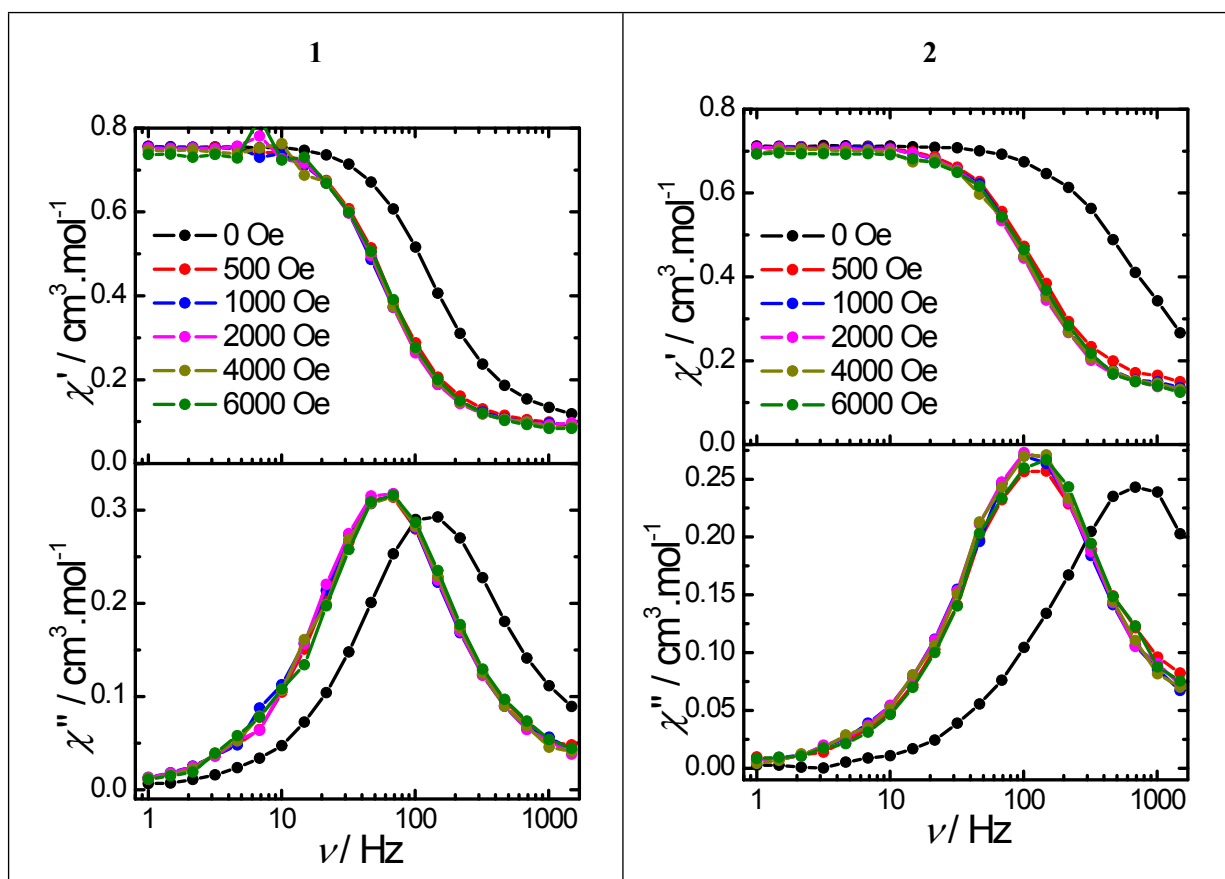


**Figure S7:** Frequency dependence of  $\chi'$  and  $\chi''$  for **1** and **2** for various dc fields at 20 K. Right: Field dependence of the relaxation time for **1** at 6 K. The red solid line represents the fit with Eq. 2.

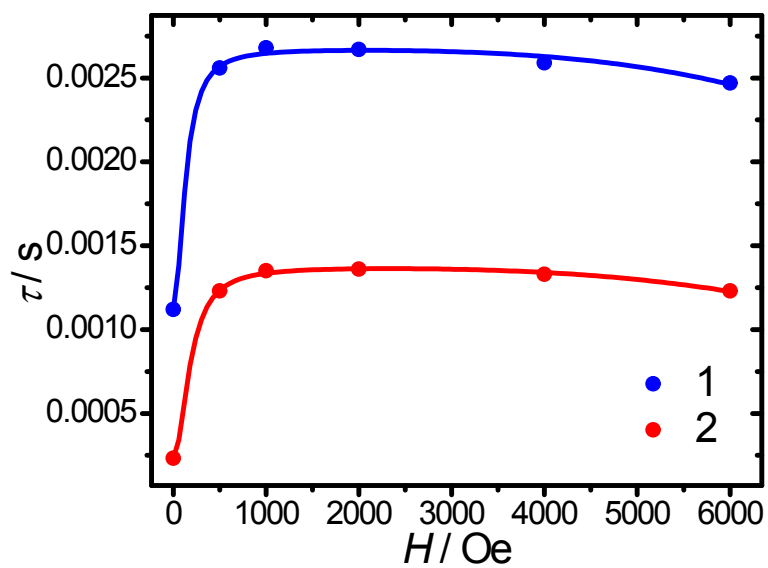


**Figure S8:** Field dependence of the relaxation time for **1** and **2** at 20 K. The red solid line represents the fit with Eq. 2.

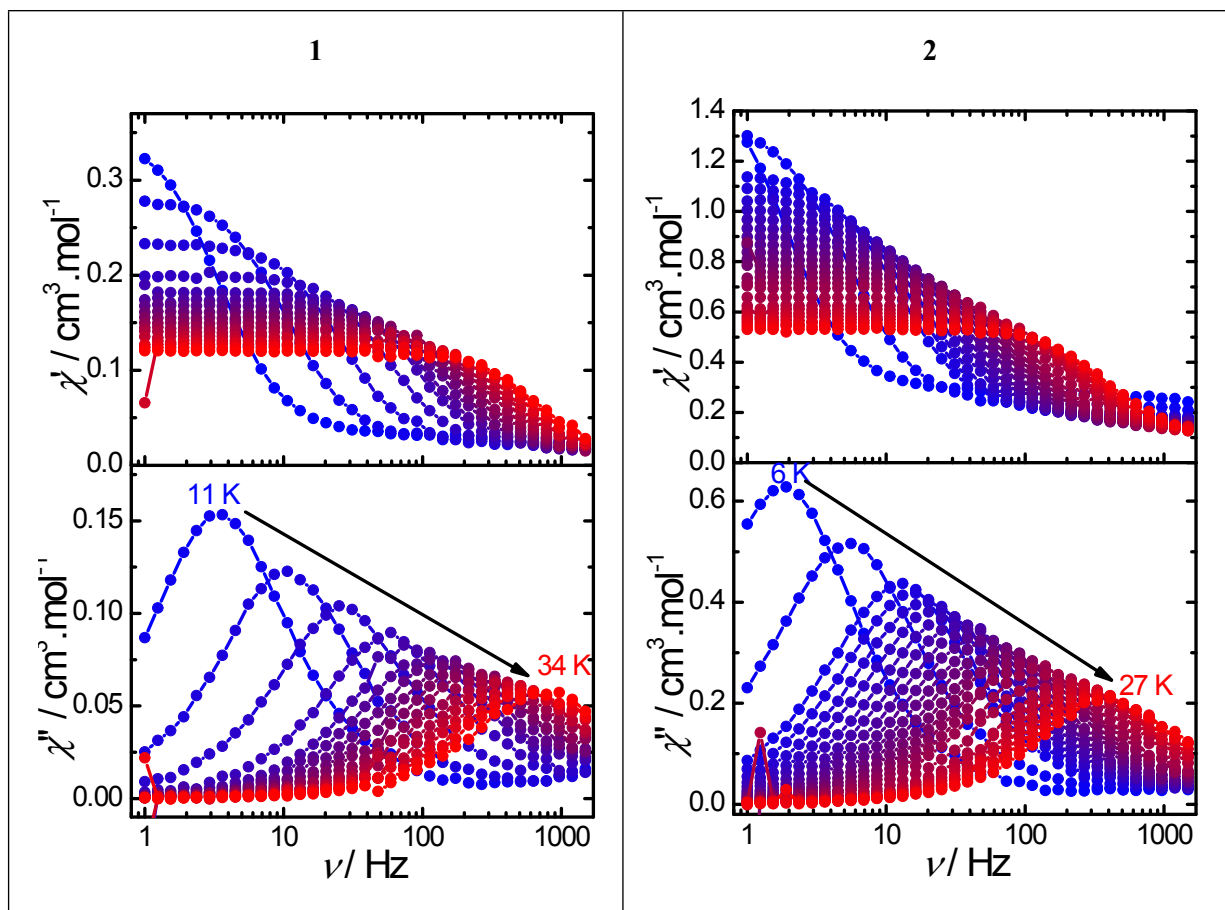


**Figure S9:** Frequency dependence of  $\chi'$  and  $\chi''$  for **1** and **2** under a 1000 Oe dc field.

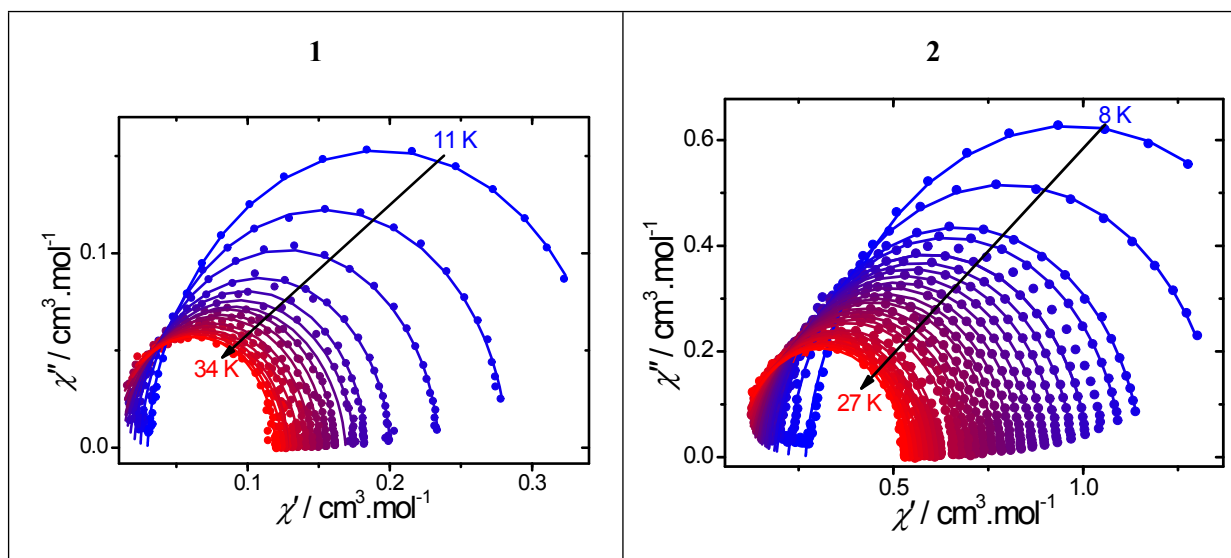


**Figure S10:** Cole-Cole (Argand) plot obtained using the ac susceptibility data for **1** (1000 Oe). The solid lines correspond to the best fit obtained with a generalized Debye model.

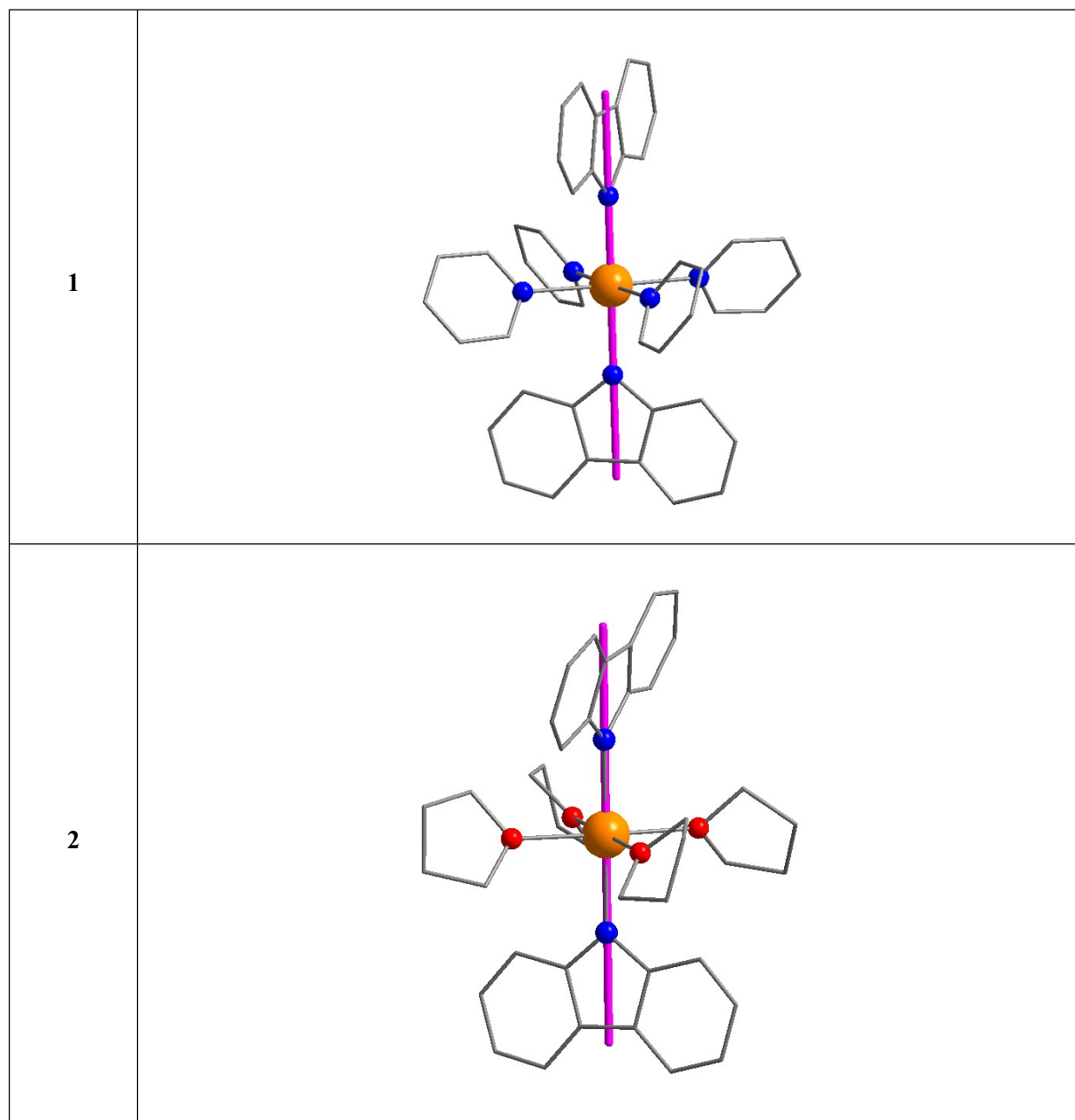


**Figure S11:** Orientation of the anisotropic axis (purple) in **1** and **2** obtained from the MAGELLAN software.

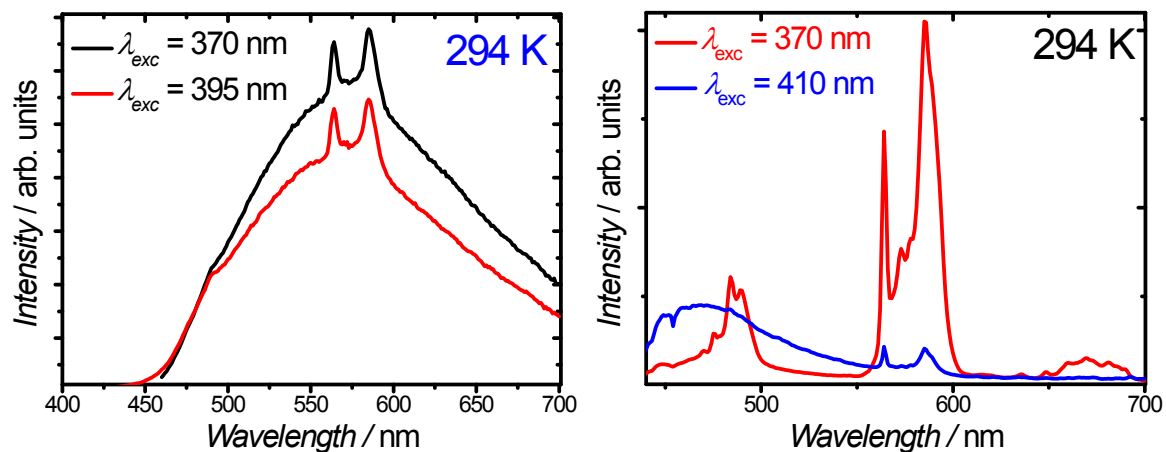


**Figure S12:** Room temperature emission spectrum for 1 (left) and 2 (right).

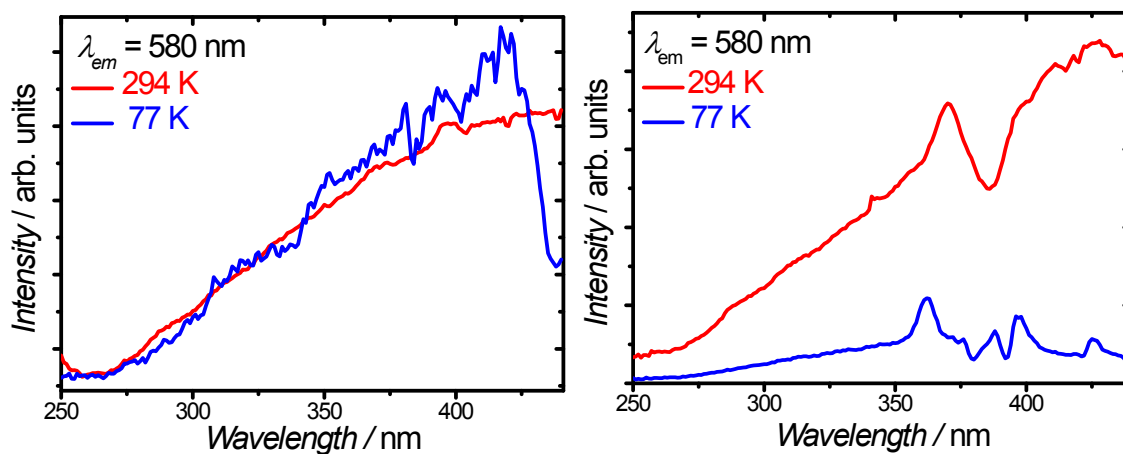


**Figure S13:** Excitation spectrum for 1 (left) and 2 (right).

**Table S1:** Crystal data, data collection and structure refinement details.

	<b>1</b>	<b>2</b>
Formula	C <sub>88</sub> H <sub>76</sub> BDyN <sub>10</sub>	C <sub>72</sub> H <sub>84</sub> BDyN <sub>2</sub> O <sub>6</sub>
MW	1446.89	1246.72
T, K	120	120
Crystal system	Orthorhombic	Trigonal
Space group	Pnma	R-3
Z (Z')	4(0.5)	18(1)
a, Å	18.2568(17)	43.568(6)
b, Å	14.3700(13)	43.568(6)
c, Å	26.520(2)	25.538(4)
α, °	90	90
β, °	90	90
γ, °	90	120
V, Å <sup>3</sup>	6957.6(11)	41980(13)
d <sub>выч</sub> , g·cm <sup>-3</sup>	1.381	0.888
μ, cm <sup>-1</sup>	11.30	8.37
F(000)	2980	11682
2θ <sub>max</sub> , °	58	50
Number of measured refl. (Rint)	82658 (0.0577)	116530(0.1025)
Number of independent refl.	9593	16419
Observed refl. with I>2σ(I)	8154	8422
Parameters	454	927
R1	0.0439	0.0495
wR2	0.0904	0.1155
GOF	1.008	1.182
Residual density, e·Å <sup>-3</sup> (d <sub>min</sub> /d <sub>max</sub> )	0.827/ -2.011	2.358/-0.625

**Table S2:** SHAPE analysis for **1**.

	HP	PPY	OC	TPR	JPPY
<b>1</b>	32.573	28.650	0.109	16.277	31.869
<b>2</b>	32.300	27.288	0.165	14.791	30.919

HP: Hexagon  
 PPY: Pentagonal Pyramid  
 OC: Octahedron  
 TPR: Trigonal Prism  
 JPPY: Johnson Pentagonal Pyramid

**Table S3:** Fitting of the Cole-Cole plots with a generalized Debye model for temperature ranging under a zero dc field for **1**.

$T$ (K)	$\chi_s$ (cm <sup>3</sup> . mol <sup>-1</sup> )	$\chi_T$ (cm <sup>3</sup> . mol <sup>-1</sup> )	$\alpha$
2	0.47573	7.001	0.22943
5	0.26844	2.92797	0.22234
8	0.19918	1.87201	0.20271
11	0.16797	1.3734	0.15791
14	0.13695	1.08286	0.12665
17	0.11861	0.89199	0.08917
20	0.09917	0.75982	0.06875
22	0.09399	0.69157	0.05012
23	0.08824	0.6629	0.0499
24	0.08386	0.63966	0.04986
25	0.08234	0.60981	0.03886
26	0.07679	0.58711	0.03779
27	0.07637	0.56592	0.03344
28	0.07139	0.54565	0.02889
29	0.07193	0.52769	0.02496
30	0.07061	0.50973	0.02192
31	0.0626	0.49495	0.02819
32	0.06352	0.47891	0.02402
33	0.05278	0.46571	0.03186
34	0.0477	0.37586	0.01966

**Table S4:** Fitting of the Cole-Cole plots with a generalized Debye model for temperature ranging under a zero dc field for **2**.

$T$ (K)	$\chi_S$ (cm <sup>3</sup> . mol <sup>-1</sup> )	$\chi_T$ (cm <sup>3</sup> . mol <sup>-1</sup> )	$\alpha$
2	0.94671	6.50025	0.22016
6	0.35088	2.28443	0.23234
10	0.23455	1.39526	0.21692
12	0.19845	1.17533	0.20849
12.6	0.20555	1.12566	0.18691
13.2	0.19361	1.06882	0.18076
13.8	0.18931	1.0222	0.16722
14.4	0.17375	0.98348	0.17257
15	0.1718	0.94451	0.15775
15.6	0.16439	0.90854	0.15446
16.2	0.14336	0.87647	0.15878
16.8	0.14448	0.84486	0.14887
17.4	0.14017	0.81749	0.14611
18	0.12632	0.7902	0.14412
18.6	0.12111	0.76728	0.14894
19.2	0.10942	0.74392	0.14744
19.8	0.10976	0.72244	0.13875
20.4	0.11027	0.70142	0.1329
21	0.11225	0.68156	0.12109
21.6	0.09078	0.66222	0.13267
22.2	0.0982	0.64669	0.11882

**Table S5:** Fit parameters of the field dependence of the relaxation time at 20 K for **1** and **2**.

<i>Compound</i>	$D$ (s <sup>-1</sup> K <sup>-1</sup> Oe <sup>-4</sup> )	$B_1$ (s <sup>-1</sup> )	$B_2$ (Oe <sup>-2</sup> )	$K$
<b>1</b> (20 K)	$1.24 \times 10^{-15}$	518.99	$1.31 \times 10^{-4}$	373.88
<b>2</b> (20 K)	$3.33 \times 10^{-15}$	3567.13	$1.68 \times 10^{-4}$	727.61



**Table S6.** Fitting of the Cole-Cole plots with a generalized Debye model under a 1000 Oe dc field for

1.

$T$ (K)	$\chi_S$ (cm <sup>3</sup> . mol <sup>-1</sup> )	$\chi_T$ (cm <sup>3</sup> . mol <sup>-1</sup> )	$\alpha$
11	0.0296	0.35708	0.04355
14	0.02461	0.28277	0.03435
17	0.02029	0.23436	0.03256
20	0.01709	0.20014	0.03041
22	0.01442	0.18353	0.03113
23	0.01197	0.1754	0.04742
24	0.01099	0.16894	0.05375
25	0.0112	0.16195	0.03619
26	0.01073	0.15595	0.03857
27	0.00769	0.15044	0.04186
28	0.00413	0.14542	0.06244
29	0.00346	0.14094	0.06259
30	0.00211	0.13611	0.06439
31	0.00578	0.12839	0.01799
32	1.7434E-4	0.12785	0.05704
33	0.00196	0.12439	0.04417
34	1.54415E-9	0.11991	0.03769

**Table S7.** Fitting of the Cole-Cole plots with a generalized Debye model under a 1000 Oe dc field for

2.

$T$ (K)	$\chi_S$ (cm <sup>3</sup> . mol <sup>-1</sup> )	$\chi_T$ (cm <sup>3</sup> . mol <sup>-1</sup> )	$\alpha$
8	0.26848	1.67121	0.07083
10	0.22275	1.37341	0.0693
12	0.19161	1.15553	0.06473
12.6	0.18493	1.1046	0.06419
13.2	0.17624	1.05621	0.06042
13.8	0.16952	1.01497	0.06146
14.4	0.16432	0.97536	0.06168
15	0.16023	0.93657	0.05488
15.6	0.15144	0.90269	0.05765
16.2	0.14646	0.8704	0.05822
16.8	0.1422	0.84033	0.05419
17.4	0.13919	0.81224	0.05497
18	0.1315	0.78665	0.05615
18.6	0.13258	0.76865	0.05118
19.2	0.12476	0.73895	0.05414
19.8	0.12281	0.71796	0.04852
20.4	0.11931	0.69736	0.04964
21	0.11393	0.67728	0.05001
21.6	0.11457	0.66065	0.04554
22.8	0.10754	0.62311	0.04324
23.4	0.10316	0.61116	0.04683
24	0.09556	0.59618	0.05561

24.6	0.0976	0.58204	0.0426
25.2	0.09409	0.56856	0.05137
25.8	0.08846	0.55691	0.05721
26.4	0.08925	0.54419	0.04738
27	0.0879	0.53212	0.0476

**Table S8.** Fit parameters of the temperature dependence of the relaxation time for **1** and **2**.

Compound	$\Delta(\text{cm}^{-1})$	$\tau_0(\text{s})$	$m$	$C(\text{s}^{-1}\cdot\text{K}^{-m})$	$A(\text{s}^{-1}\cdot\text{K}^{-1})$
<b>1</b> (1000 Oe)	$89 \pm 7$	$(2 \pm 1) \times 10^{-5}$	5*	$(6 \pm 1) \times 10^{-5}$	$2 \times 10^{-21}$
<b>2</b> (2000 Oe)	$52 \pm 3$	$(7 \pm 1) \times 10^{-5}$	5*	$(1.22 \pm 0.05) \times 10^{-10}$	$1.8 \pm 0.5$

\* fixed parameter

**Table S9.** Fit parameters of the temperature dependence of the relaxation time for **1** and **2**.

Compound	$\Delta(\text{cm}^{-1})$	$\tau_0(\text{s})$	$m$	$C(\text{s}^{-1}\cdot\text{K}^{-m})$	$A(\text{s}^{-1}\cdot\text{K}^{-1})$
<b>1</b> (0 Oe)	79.9 <sup>a</sup>	$(2.0 \pm 0.8) \times 10^{-5}$	4.2 <sup>b</sup>	$0.0014 \pm 0.0002$	-
<b>1</b> (1000 Oe)	79.9 <sup>a</sup>	$(2.2 \pm 0.2) \times 10^{-5}$	5.1 <sup>b</sup>	$(5.0 \pm 0.3) \times 10^{-5}$	-
<b>2</b> (0 Oe)	28.8 <sup>a</sup>	$(2 \pm 1) \times 10^{-4}$	3.3 <sup>b</sup>	$0.13 \pm 0.01$	-
<b>2</b> (2000 Oe)	28.8 <sup>a</sup>	$0.02 \pm 0.01$	4.3 <sup>b</sup>	$0.00181 \pm 0.000007$	-

<sup>a</sup> fixed parameter from the linear fit.<sup>b</sup> to avoid overparametrization, the  $m$  values was successively fixed to different values until getting the best fitting coefficient.

## References

- 1 S. Harder, C. Ruspic, N. N. Bhriain, F. Berkermann and M. Schürmann, *Zeitschrift für Naturforschung B*, 2008, **63**, 267-274.
- 2 S. J. Lyle and M. M. Rahman, *Talanta*, 1963, **10**, 1177-1182.
- 3 Bruker, *SADABS*, 2001, B. A. Inc., Madison, Wiscosin, USA.
- 4 G. Sheldrick, *Acta Crystallographica Section A*, 2008, **64**, 112-122.
- 5 G. M. Sheldrick, *Acta Crystallogr., Sect. C: Struct. Chem.*, 2015, **71**, 3-8.
- 6 A. Spek, *Acta Cryst. C.*, 2015, **71**, 9-18.
- 7 A. Spek, *Acta Cryst. D.*, 2009, **65**, 148-155.
- 8 G. Sheldrick, *Acta Crystallographica Section A*, 2015, **71**, 3-8.

